

19 - SMALL LAMINAR BLANKS AT SIUREN I ROCKSHELTER: TECHNOLOGICAL & COMPARATIVE APPROACH

Nicolas ZWYNS

During the last two decades, a great emphasis has been brought on the production of small laminar elements among Upper Paleolithic assemblages of Eurasia. Bladelet and microblade technological systems have been described within various techno-complexes, such as Aurignacian, Gravettian, Proto-Solutrean and Magdalenian in Central and Western Europe (Aubry *et al.* 1995; Lucas 1997; Bon 2002; Bordes & Tixier 2002; Langlais 2004; Bordes 2005; Flas *et al.* 2006; Klaric 2006; Michel & Pesesse 2006; Pottier 2006; Teyssandier 2006; Teyssandier *et al.* 2006), and Early Ahmariian, Aurignacian and Kebaran in the Near-East (Chazan 2001; Monigal 2003; Williams 2003; Goring-Morris & Davidzon 2006; Lengyel 2007). Based on the material from South-Western Europe, some researchers have rehabilitated the distinction between Proto-Aurignacian, the Early Aurignacian, and subsequent Evolved Aurignacian. Mainly by stressing techno-economic differences in the production of small laminar elements, they have confirmed the existence of a variant prior to the 'Aurignacian I'. The latter is similar to the Proto-Aurignacian, an entity previously identified in Southern Europe mainly on a typological basis (Laplace 1966b; Broglio *et al.* 1996; Broglio *et al.* 2005). This distinction has been sometimes interpreted as reflecting regional variability (Bon 2002), but also as illustrating a diachronic pattern (Bordes 2005; Mellars 2006b; Teyssandier 2006). Stratigraphic successions such as Proto-Aurignacian/Early Aurignacian (e.g. Esquicho Grapaou, Abri Mochi, Le Piage, Labeko Koba, Isturitz, L'Arbreda, Cueva Morin) and Early Aurignacian/Evolved Aurignacian (e.g. Caminade-Est, Abri Pataud, Cueva Morin), have been documented in several sequences (Maroto *et al.* 1996; Kuhn, & Stiner 1998; Soler 1999; Bazile 2002; Kuhn 2002; Arrizabalaga *et al.* 2003; Chiotti 2003; Bordes 2005; Maillo Fernandez 2005; Teyssandier *et al.* 2006; Normand *et al.* 2007; Bordes *et al.* 2010).

Against the odds, small laminar elements have turned out to be influential in larger debates, leading to the re-assessment of interpretative models such as the development of the Aurignacian techno-complex, or shifting pre-existing models of Anatomically Modern Humans (AMH) dispersal to the Proto-Aurignacian. The proposed models of AMH dispersal point out two main different routes leading to Europe (Bar-Yosef 2002; Mellars 2006b). In the Northern route scenario, Eastern Europe is colonized from the western ridge of the Black Sea.

However, such models are raising a number of issues regarding direct inter-regional comparisons between lithic assemblages (Tsanova *et al.* in press). The techno-economic, typological and metric attributes of the small laminar products remain difficult to compare with the Western and Central European records. This situation is partly due to the scarcity of multilayered Aurignacian sites eastward of the Carpathian mountain range, but also because of numerous theoretical and methodological differences between scholars.

In this context, the Siuren I rockshelter is of great interest as it has yielded three distinct cultural units attributed to the Aurignacian technocomplex *sensu lato*, giving us the opportunity to perform a detailed technological description of the material and to compare our results with the existing data set.

Sampling and measurement

In order to outline the major trends of the small laminar elements production, we sampled sub-levels Fb1, Fb2, Gc1-Gc2, and Unit H, trying to obtain a relevant and representative picture of the technological traits expressed in the assemblages. The material is classified here by arbitrarily defined categories (tabl. 1, fig. 6). The bladelet category groups all laminar elements with widths smaller than 12mm and larger than 6 mm, while the microblades category groups elements with a width smaller than 6 mm¹. The sample analyzed for sub-level Fb1 is an exhaustive selection including all cores, retouched and non-retouched blanks available, with the exception of a few problematic fragments². Sub-level Fb2 has yielded more than a thousand unretouched elements, just a few displaying secondary treatment. Regarding the unretouched blanks, we consider here the sample from Fb1 very similar to Fb2 and sufficient for the purpose of this analysis. The material from sub-levels Gc1-Gc2 and Unit H

¹ Although our total counting of artifacts is in overall agreement with those mentioned in other chapters (Demidenko, Chabai, this volume), small differences in number of elements within sub-categories may occur. This is partly due to the measurement method, Y. Demidenko and V. Chabai measuring the width in the middle of the piece.

² Were considered here only cores on which technological features, such as multiple laminar removals, could still be observed at the time of discard.

	Fb1		Fb2		Gc1-Gc2		H	
	n	%	n	%	n	%	n	%
bladelet	135	34%	0	0%	277	59%	61	44%
retouched bladelet	2	1%	8	14%	40	8%	16	12%
microblade	242	62%	0	0%	96	20%	33	24%
retouched microblade	14	4%	48	86%	58	12%	28	20%
	393	100%	56	100%	471	100%	138	100%

Table 1 - General composition of the blank sample.

	n	%
Fb1	5	21%
Fb2	8	33%
Gb1-Gb2	2	8%
Gc1-Gc2	4	17%
Gd	1	4%
H	4	17%
	24	100%

Table 2 - Cores included in the sample.

is here entirely represented, with the exception of a few problematic elements and with the typical burin spalls that might have been sources of bias. In addition, we studied cores from sub-levels Gb1-Gb2, Gb2a and Gd (tabl. 2). We will not analyze blade production here although relationships between the production systems will be discussed in the concluding paragraphs.

The sample considered is described according to technological and metric attributes to provide a realistic picture of its internal variability. The attribute list is composed of quantitative (measurement) and qualitative (e.g. type of platform, type of profile, conservation) data. The length was measured only when laminar elements were complete; width and thickness are always measured at their maximum (fig. 1). Platform surfaces are measured in length and width. Profiles are qualitatively described following a classification adapted from previous studies (Bon 2002). Only blanks which are twisted until their mid-section will be considered as such. Cores are described according to their technological features, and typologically categorized independently afterward (fig. 2)

We use box-plot and bag-plot charts to distinguish the main trends among a sample. These charts are constructed around a median value and therefore, identify outliers that could be sources of bias. We use the Mann-Whitney U-test to compare measurements as it allows comparisons between two different sample sizes. When applying Shapiro-Wilk test, most of the samples appear as non-normally distributed. They show, however, skewed unimodal distributions close to the normal fit. We use one-way Anova and Tukey’s pairwise comparisons to compare means.

Sub-level Fb1

Cores

Among the five cores analyzed in unit Fb1 (fig. 3), three were produced on small sized pebbles/nodules and two on flake

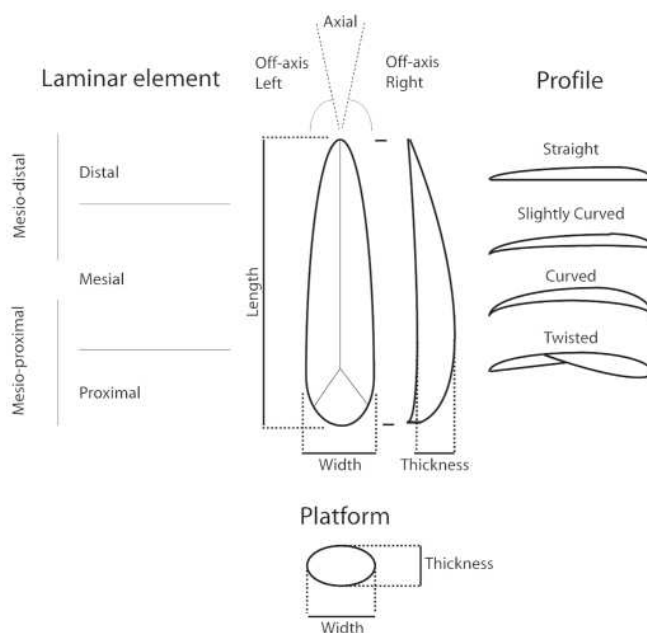


Figure 1 - Measurement methodology.

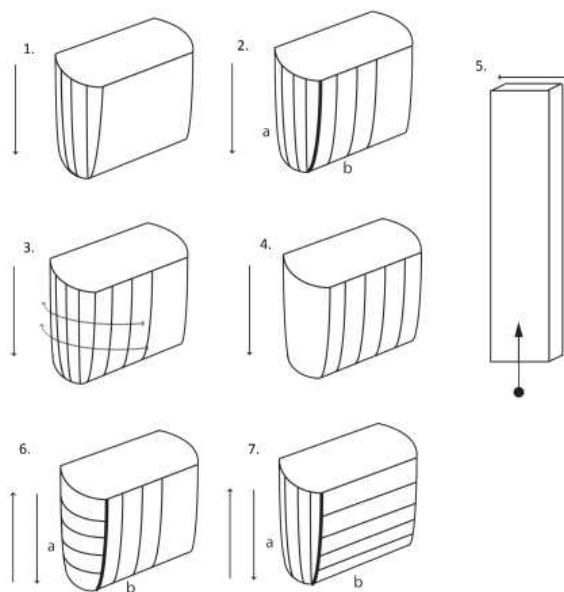


Figure 2 - Core morphology. 1-2, frontal reduction; 3, semi-tournant; 4, reduction starting from the broad face; 5, burin, removals perpendicular to the longitudinal axis; 6-7, orientation change.

blanks. Among the three cores on pebbles, two are *semi-tournant* starting the reduction from the narrow edge of the block, the third one showing two separate flaking surfaces, testifying to a change of orientation over the course of the reduction process. The two cores on flakes display unidirectional frontal and *semi-tournant* reduction patterns, both starting from the narrow edge of the blank slightly expanding on the wide face. The frontal reduction takes place perpendicularly to the flake’s long axis. All cores show a plain striking platform, only one being reshaped by a tablet removal. Although they were discarded, four cores of the five retain traces of a thin abrasion on the external ridge

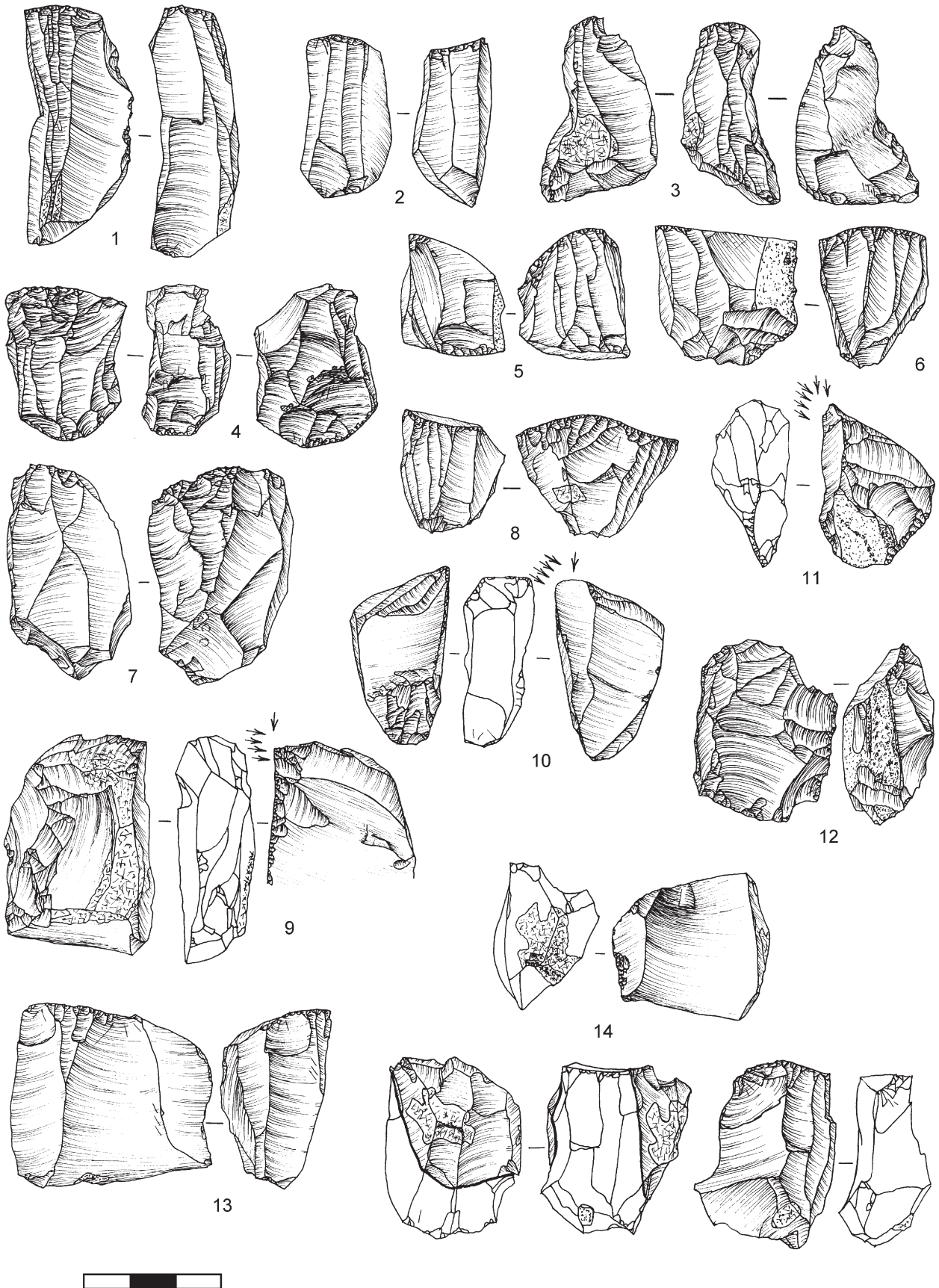


Figure 3 - Cores from sub-levels Fb1&Fb2 (illustrations borrowed with the courtesy of Y. Demidenko).

of their striking platform. All of the complete last removals observed on the core flaking surfaces show a twisted profile combined with an off-axis orientation. Those blanks have lengths between 16 and 26 mm and widths between 3 and 8.5 mm. Flaking surfaces are of a triangular shape due to the convergent orientation of the removals. Their proportions vary between 23 and 27 mm in length and between 7 and 21 mm in width. Only one artifact shows a shorter flaking surface (12 mm length), perhaps due to reduction effects. Lateral management flakes were detached from the striking platform except in one case, for which the flakes were removed from the distal end of the core. From a typological point of view, two cores can be classified as carinated endscrapers, and two as carinated burins (Demars, & Laurent 1992), the remaining item being categorized as a prismatic core.

Laminar blanks

When we compare the samples of unretouched and retouched elements, we observe a similar distribution although retouched blanks are more clustered. Unretouched elements show a mean of 5.7 mm width with a standard deviation of 2.2 mm. Retouched elements show a mean of 4.9 mm width and a standard deviation of 1.6 mm. These two samples belong to the same population (Mann-Whitney, $T=UB=2416$, $p=0.18$) (fig. 4-5).

Most of the Fb1 laminar elements show oblique external platform angle, the external ridge systematically showing traces of abrasion. In spite of their small size, artifacts display macroscopic lips on their platform internal ridge. Platforms are plain, showing a thickness of 0.5 mm maximum and a width ranging between 0.1 and 3.5 mm.

Dorsal scars show a majority of unidirectional removals, and when preservation allows us to observe it, a clear trend toward a convergent orientation. Sections are triangular or trapezoidal, with only in a few cases rectangular (naturally backed or *pan revers*).

While the profiles of non-retouched elements seem to be equally represented, the situation is different when looking only at retouched tools. As previously noted (see tabl. 1), almost exclusively microblades have been retouched. Twisted elements represent half of the sample. The curved, slightly curved and straight elements are then equally represented (fig. 6). However, when looking at the orientation of retouched elements, we observe that 10 artifacts out of 14 are off-axis, 2 being axial and 2 others undetermined. Moreover, twisted elements are systematically combined with the off-axis character.

The retouched microblades (fig. 7 & 8) show a majority of direct retouch ($n=7$), directly followed by inverse retouch ($n=6$), only one with alternate retouch. Among the artifacts with direct retouch, some are backed combining 90 degrees marginal steep and semi-steep retouch (2 microblades and 1 bladelet) on the right edge, others show a combination of thin and semi-steep retouch on the right edge ($n=4$), only one showing retouch on the left distal end. Artifacts displaying inverse retouch show mainly thin retouch but also a combination of marginal thin and semi-steep retouch on the right edge ($n=4$), but also on the

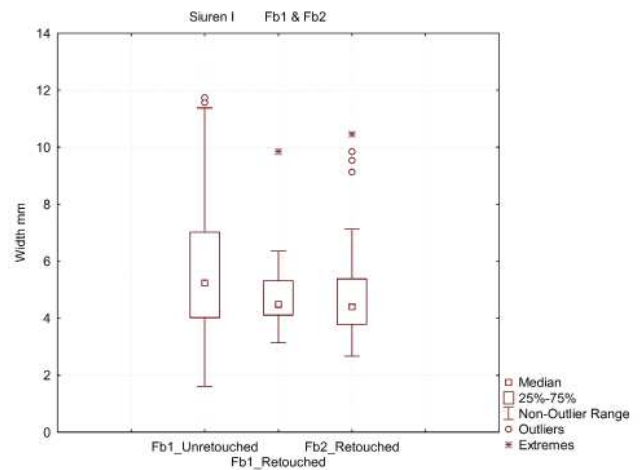


Figure 4 - Box-plot comparing the width distribution between unretouched and retouched elements from sub-level Fb1 and retouched elements from sub-level Fb2. Whiskers are drawn from the top of the box up to the largest data point less than 1.5 times the box height (upper inner fence). The circles represent values which are outside the upper inner fence, considered here as outliers.

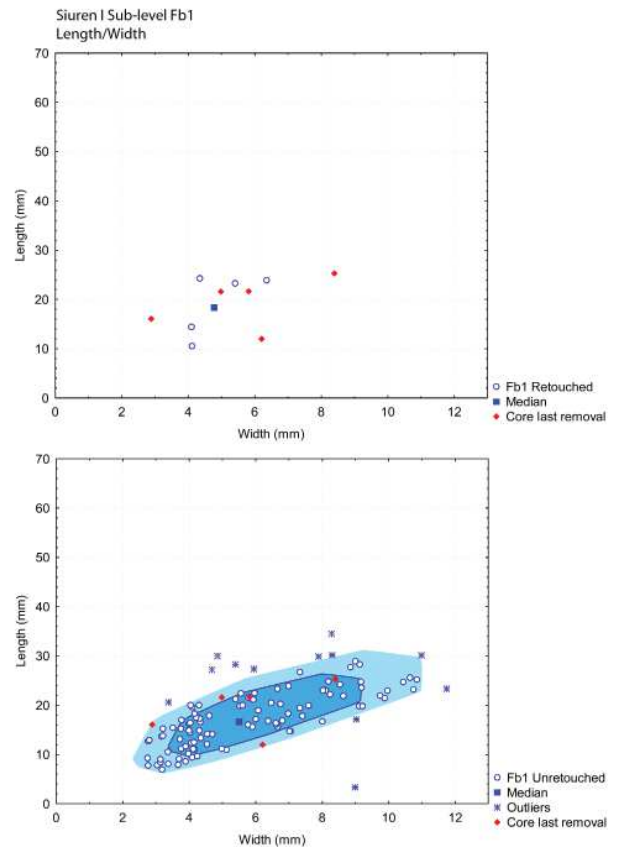


Figure 5 - Bag-plot chart showing the length/width distribution of retouched and unretouched elements from sub-level Fb1, compared with the complete last removals observed on the cores. The dark circle (bag) represent 50% of the observations with greatest bivariate depth. The light circle (loop) represent three times the bag (fence).

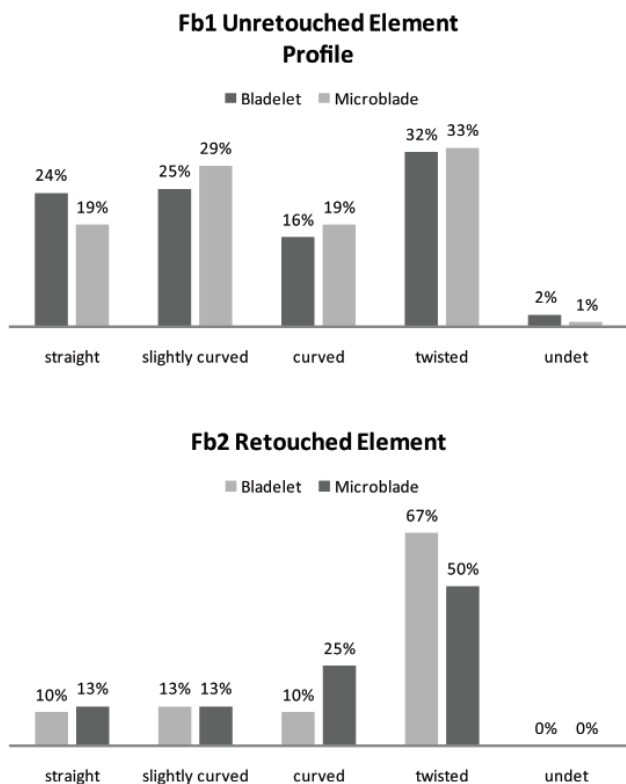


Figure 6 - Sub-levels Fb1&Fb2, laminar element profiles.

left edge (n=2). These artifacts can be classified typologically as Dufour microblades. However, the Dufour *Roc-de-Combe* sub-type, defined as showing a combination of twisted profile and inverse or alternate retouch (Demars & Laurent 1992), is almost absent. If the general morphology of the Dufour microblades comes close to this sub-type, it is by their metric attributes and their off-axis orientation. Actually, only one Dufour microblade displays a clear twisted profile. The single retouched bladelet of the Fb1 sample has a combination of thin and semi-steep direct retouch along the mesio-distal end.

Sub-level Fb2

Generally speaking, Unit Fb2 show strong affinities with Unit Fb1. Retouched bladelets (n=5), retouched microblades (n=51) and cores (n=9) have been analyzed here.

Cores

Five of the cores (fig. 3) are produced on small nodules, three on laminar flakes and one on flake. Six cores show unidirectional removals, five of them following a frontal reduction pattern, only one of them extending slightly on the wide side. Two cores display opposed striking platforms on the narrow edge, the removals following the long axis of the piece. One artifact shows two separate flaking surfaces as the result of a change of orientation over the course of reduction. The external platform

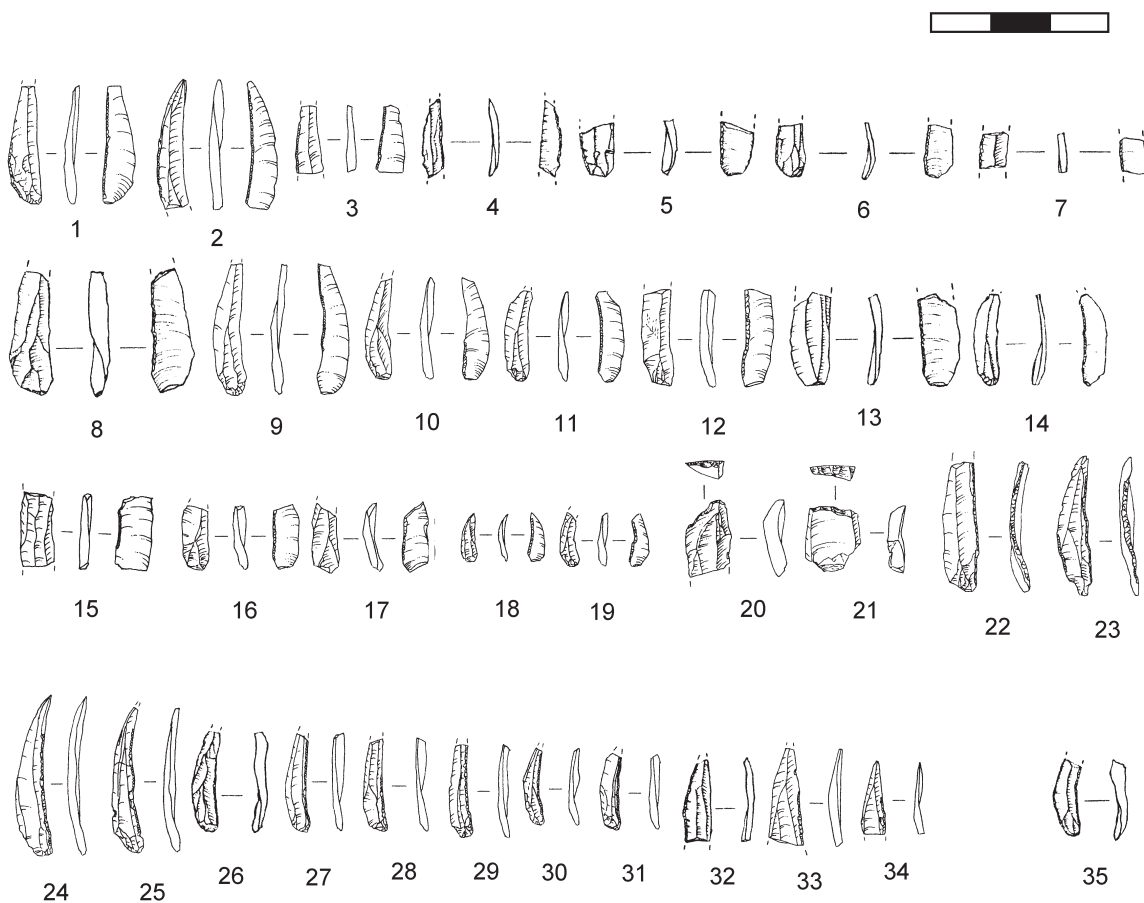


Figure 7 - Retouched bladelets and microblades from sub-levels Fb1 and Fb2 (illustrations borrowed with the courtesy of Yu. E. Demidenko).

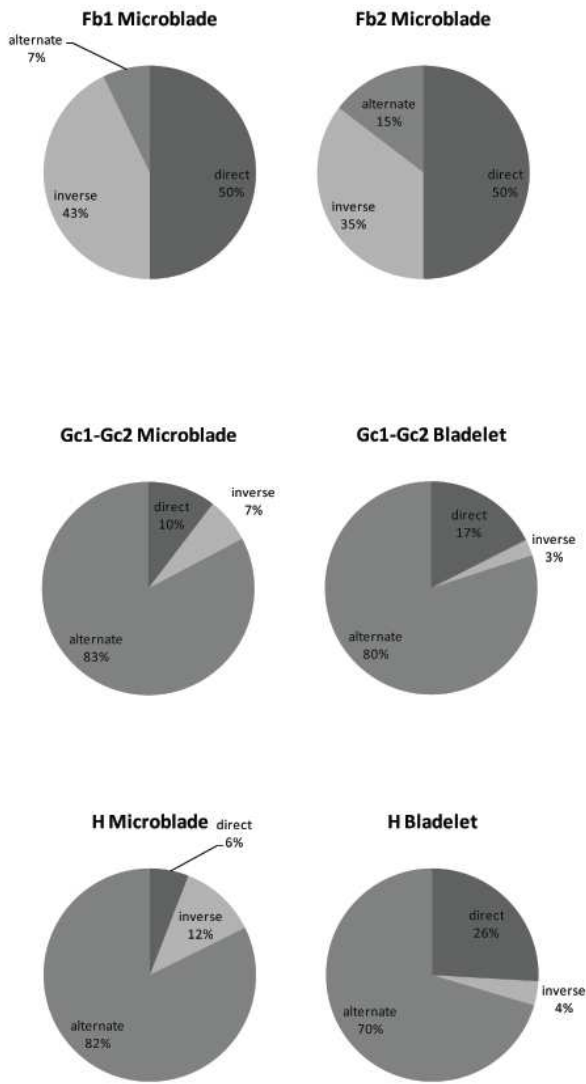


Figure 8 - Retouch location charts.

angle is oblique and the external ridge shows traces of abrasion. The preserved striking platforms are plain. Flaking surface management is sometimes achieved by the removal of an overshoot from the striking platform, and lateral management is mainly performed by flake removals from the striking platform. All observed removals on flaking surfaces show a convergent orientation. From a typological point of view, cores can be classified as carinated burins (n=2), as core-burin (n=1), carinated endscraper (n=1), shouldered endscrapers (n=2), and busked burin (n=1) (de Sonneville-Bordes & Piveteau 1960; Demars & Laurent 1992) (fig. 9). The latter is a produced on a secondary crested blade. One end displays lateral removals perpendicular to the blank's long axis. Removals are stopped by a notch which is surrounded by small retouch. The last microblade removed some of these retouch scars and one of the negatives on the ventral face seems to indicate similar preparation in the earliest stages of the reduction³. The opposite end shows chips removals ending with an endscraper morphology.

³ This indicates that the last microblade removal occurred after the production of the notch (Flas *et al.* 2006).

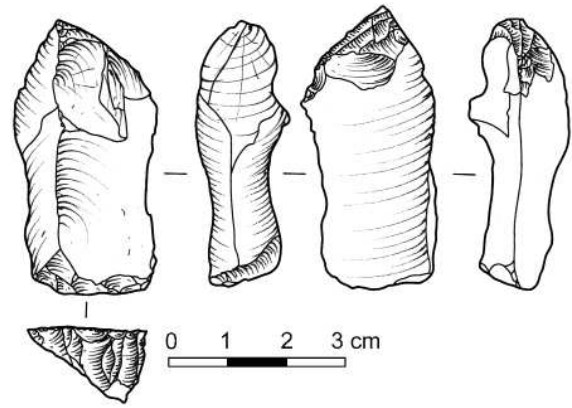


Figure 9 - Sub-level Fb2, Busked burin (drawing by N. Zwyns).

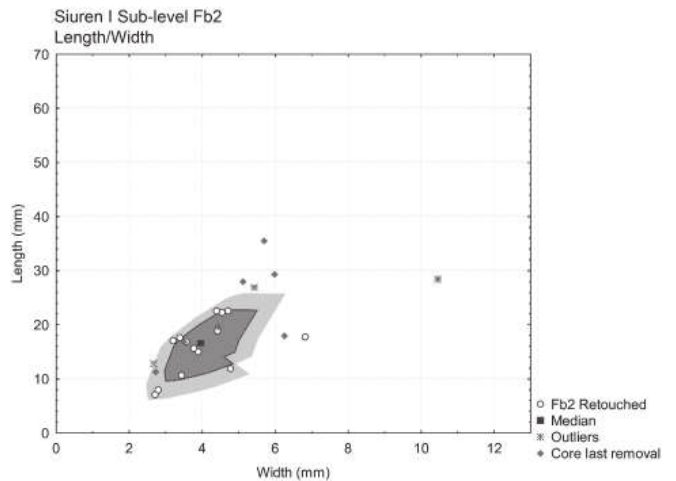


Figure 10 - Bag-plot chart showing the length/width ratio of retouched elements from sub-level Fb2, compared with the length/width ratio of the complete last removals observed on the cores. The dark circle (bag) represent 50% of the observations with greatest bivariate depth. The light circle (loop) represent three times the bag (fence).

Laminar blanks

The mean of width measurement is 4.7 mm with a standard deviation of 1.6 mm (figs. 4 & 10). Following the conventional definition, we observe 5 retouched bladelets. Two are of curved profiles, one is slightly curved, one is straight and one is twisted. Three are off-axis, one is axial and one profile remains undetermined. All of them have direct thin/semi-steep retouch. Three of these bladelets have distal retouch somewhat similar to a small truncation, one has a continuous retouch along the right edge and one has proximal retouches on the right edge. Only one is complete with a length of 28 mm. Platforms are plain and abraded on their external ridge and show macroscopic lips.

The retouched microblades (n=51) are clearly dominated by twisted elements, other types of profiles being equally under-represented (fig. 6). They are transformed by a combination

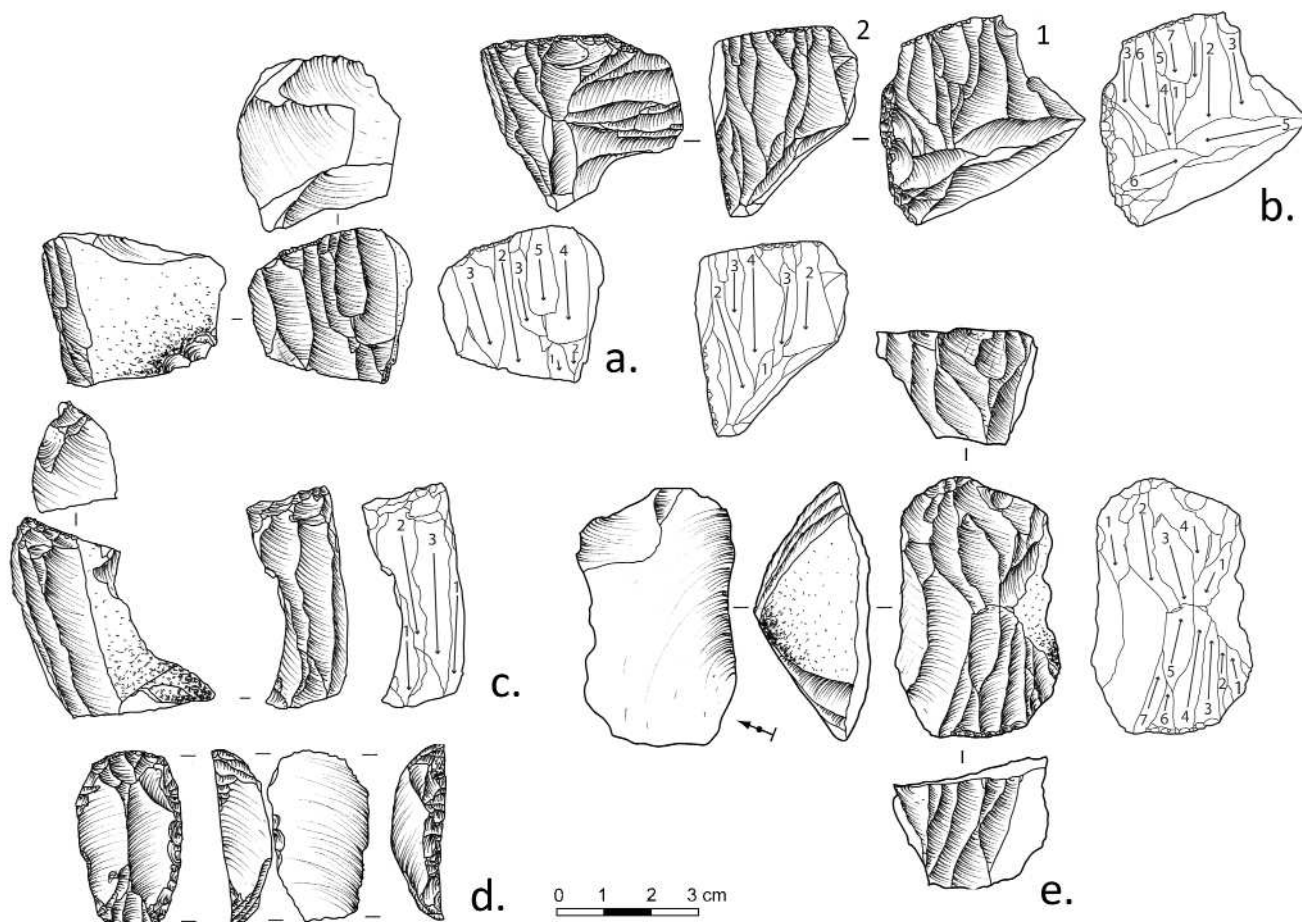


Figure 11 - Unit G, Cores and diacritic reconstruction. The different phases illustrate the chronology of removals; d, endscraper (drawing by N. Zwyns).

of thin and semi-steep retouch. Blanks displaying direct and inverse retouch are almost equally represented with only a few of them showing alternate retouch (fig. 7 & 8). Microblades showing inverse and alternate retouch are typologically classified as Dufour and represent half of the retouched microblades ($n=26$). Among those Dufour microblades, 19 of the 26 can be assigned to the *Roc-de-Combe* subtype ($n=19$). The Dufour microblades show a clear pattern of retouch location. Inverse retouch are systematically located along the right edge, and for alternate retouch, direct retouch always follows the left edge. However, artifacts with only direct retouch do not show such a pattern. It is noteworthy that the majority of microblades with direct retouch are also produced on twisted blanks, and that almost all of the retouched blanks are off-axis.

Sub-levels Gc1-Gc2

The sub-levels Gc1-Gc2 material represents the largest sample studied in this series. A total of 471 laminar elements and 3 cores were analyzed, 40 retouched bladelets and 58 retouched microblades. We also studied retouched laminar elements and cores from sub-levels Gb1-Gb2 and Gd. Although bladelets and microblades are not presented here, they are considered similar to Gc1-Gc2. Four additional cores associated with these sub-levels are described below.

Cores

Although the sample is rich in laminar blanks, the frequency of core-like elements is rather low. Three of the cores are produced on flake or laminar flake blanks, three are on small blocks, and one is on a thin slab (figs. 11 & 12). All cores are unidirectional, worked on both narrow and wide surfaces. Three of the cores show a change of orientation during the course of reduction, with a flaking surface sometimes perpendicular to the previous one (figs. 11b, 12h, 12i). Diacritic reconstructions show the chronology of removals and underline the absence of genuine bi-directionality. Preparation of the flaking surfaces is achieved by lateral overshoot/plunged removals or by divergent removals from an opposed platform, giving a triangular shape to the distal part of the flaking surface.

The platform is plain or sometimes reshaped by a tablet removal. Abrasion is still present on the external ridge after the discard. Last removals are between 10 and 44 mm in length for 4.5 to 7.3 mm in width, showing curved or slightly curved profiles (see fig. 12i). Removal scars show a convergent orientation; only one core displays parallel scars. Five of the cores can be classified as prismatic (two of them showing a 90 degrees change of orientation). Two artifacts can be classified as carinated endscrapers. The first one is a bladelet core with two

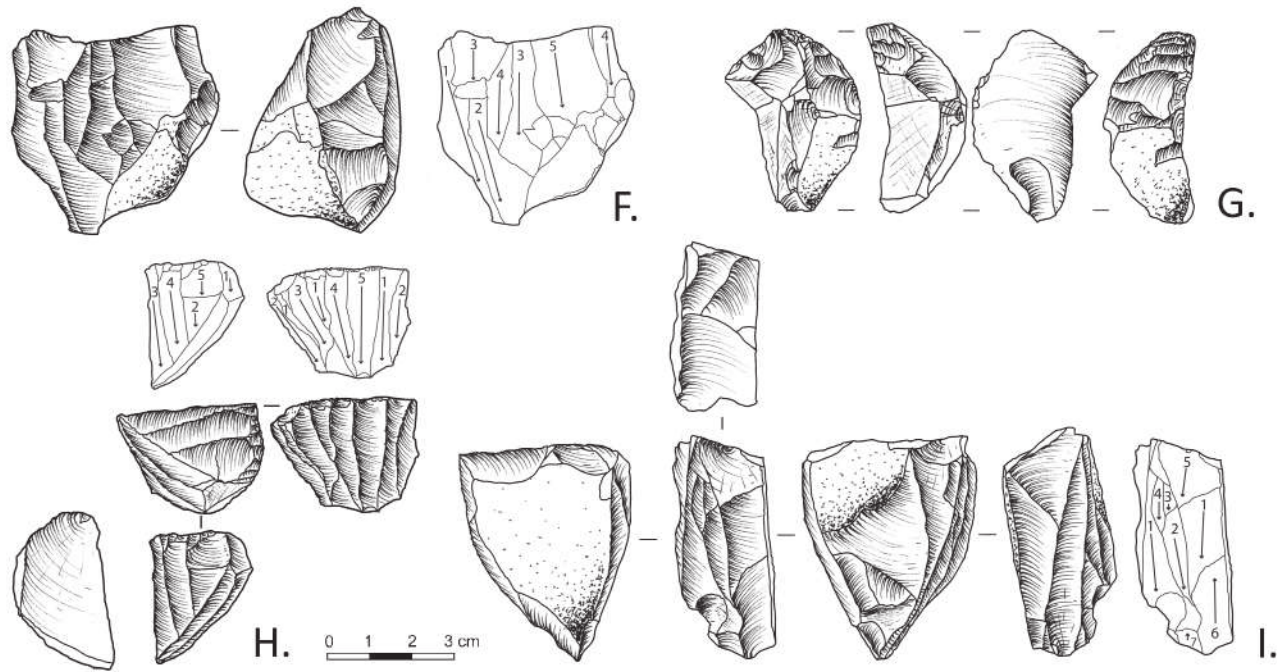


Figure 12 - Unit G, Cores and diacritic reconstruction. The different phases illustrate the chronology of removals (drawing by N. Zwyns).

separate flaking surfaces, taking place on both ends of the blank (double endscraper) (fig. 11e). Diacritic reconstruction shows the exploitation of one side after the other. The second one is smaller but similar in the general morphology (fig. 11d). It is either a tool the result of a sharp reduction or the expression of a need to produce very small blanks. One core has been classified as an atypical carinated endscraper, the last removals being more flakes than bladelets (fig. 12g) (de Sonneville-Bordes & Perrot 1954). The last one is a core on the narrow ridge of a slab, with two consecutive flaking surfaces. Removals in the opposite direction prepare a new striking surface, giving the appearance of bidirectionality (fig. 12i).

Laminar blanks

The unretouched elements have a mean of width measurement 7.8 mm (standard deviation of 2.3 mm) and retouched elements show a mean of 6 mm (1.8 mm of standard deviation) (figs. 13 & 14). Retouched and unretouched elements display an asymmetric distribution and are statistically different (Mann-Whitney, $T=UB=9.632^{12}$, $p<0.01$).

Platforms are plain and show a sharp angle with the ventral face, most of them being lipped with their external ridge bearing traces of abrasion. Dorsal scars are unidirectional and sub-convergent. Profiles show a clear trend toward the production of straight elements, followed by slightly curved and curved elements. The twisted elements are virtually absent. This pattern can be observed among retouched and un-retouched elements, bladelets or microblades (fig. 15).

The set of bladelets is largely dominated by alternate retouch (80%), followed by direct (17%) and inverse retouch (3%) (figs. 8 & 16). The same trend can be observed among the microblades, alternate retouch dominating the set up to 83%. So most of the

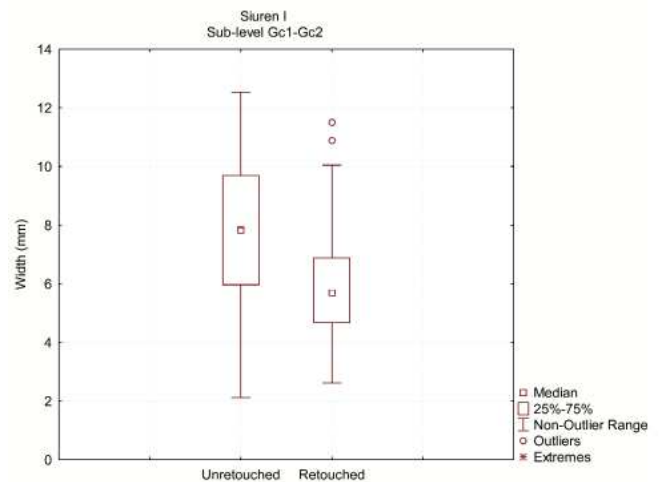


Figure 13 - Box-plot comparing the width distribution of unretouched and retouched elements from sub-level Gc1-Gc2. Whiskers are drawn from the top of the box up to the largest data point less than 1.5 times the box height (upper inner fence). The circles represent values which are outside the upper inner fence, considered here as outliers.

laminar elements display either inverse or alternate retouch can be classified as Dufour and are produced on curved, slightly curved and straight profile blanks (Demars & Laurent 1992). When observable, most of the Dufour are axial. They show a clear pattern of secondary treatment, inverse retouch following the right edge and direct retouch following the left edge (32 out of 32 Dufour bladelets, and 42 of 42 Dufour microblades bearing alternate retouch, 3 of the 4 with inverse retouch). The most common type of retouch is a combination between thin and semi-steep retouch with the inverse retouch tending to be more flattened. Three fragments of Dufour show a tip pointed by alternate retouch.

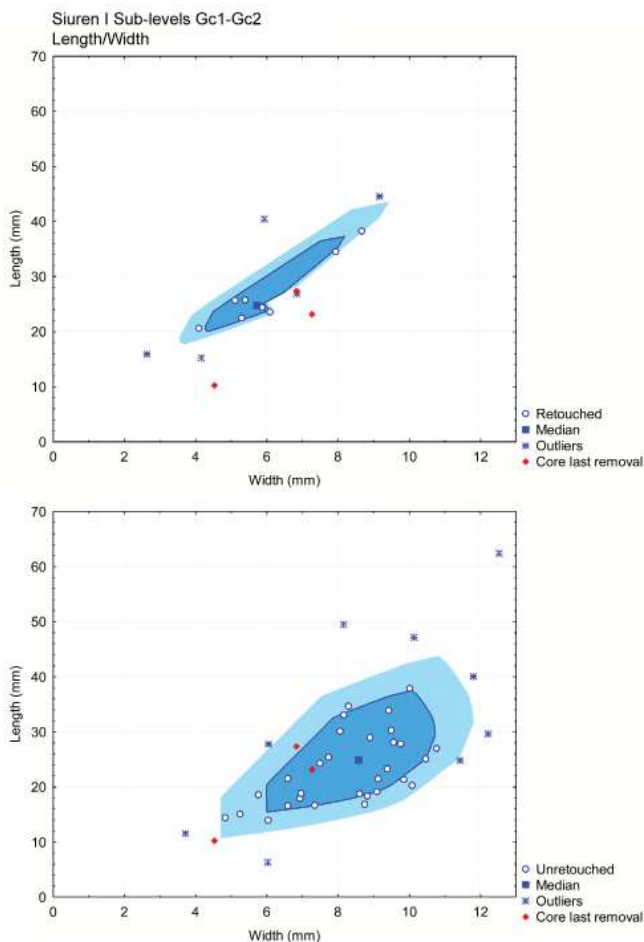


Figure 14 - Bag-plot chart showing the Length/Width distribution of retouched and unretouched elements from sub-level Gc1-Gc2, compared with the complete last removals observed on the cores associated with those sub-levels. The dark circle (bag) represent 50% of the observations with greatest bivariate depth. The light circle (loop) represent three times the bag (fence).

We observe lateral damages on some of the Dufour elements, mostly affecting the ventral face along the edge opposed to the retouch (e.g. figs. 16:8-9, 12, 14, 22). A small number of the breakage pattern is similar to experimental impact breakage (Fischer *et al.* 1984).

Artifacts with direct retouch show no pattern of transformation, half of them displaying bilateral retouch. Three of these fragments are clearly typed as Font-Yves/Krems and at least two more likely belong to this category as well. One additional distal fragment is of asymmetrical morphology, thin retouch follow the left edge as steep retouch crops the blank (fig. 16:34).

Unit H

Cores

Four cores are described here. One is made out of a block, one is on a laminar blank, the rest on unidentified blanks (fig. 17). Two of the cores have unidirectional removals on their flaking surface and follow a frontal reduction pattern. Striking platforms are flat or reshaped by tablet removals; three of the cores

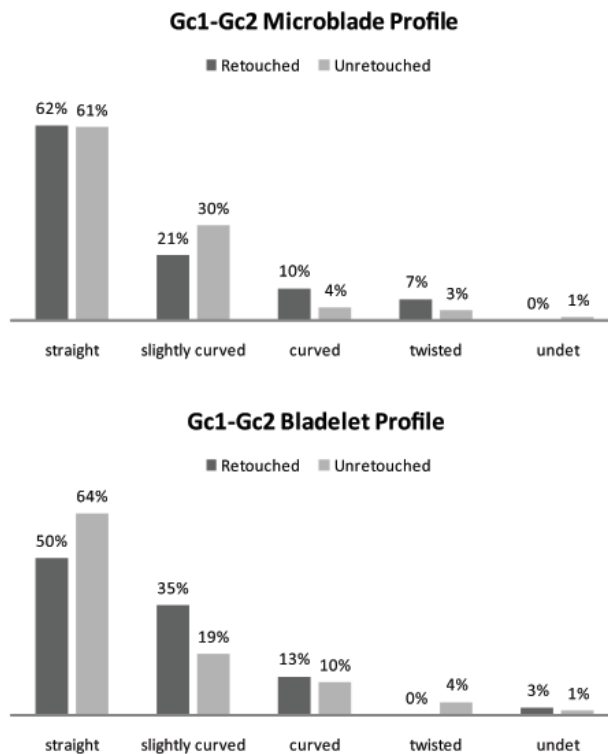


Figure 15 - Sub-levels Gc1-Gc2, laminar element profiles.

still show traces of abrasion on their external ridge. External platform angles are oblique. The flaking surfaces are triangular; shaped either by the convergent removals, management over-shot and plunged removals, distal shaping, or the preparation of the sides of the core. Diacritic reconstructions show mainly frontal reduction. Although one core seems to be *semi-tournaant*, it was difficult to convincingly demonstrate this without refits (fig. 17c). One core is clearly on the edge of the conventional definition of bladelet, the last removal width being of 11.9 mm (fig. 17d). This core is likely to be linked with a larger blade reduction sequence. Three of these cores can be classified as prismatic. The remaining core is produced on a neo-crested blade following a frontal reduction pattern along the longitudinal axis of the blank and could be considered as a carinated endscraper (fig. 17a). Another core can be typed as a *robot* or carinated endscraper (Demars & Laurent 1992) (fig. 17b).

Laminar blanks

The mean of unretouched elements is 7.8 mm (with 2.3 mm of standard deviation) but when we consider only the retouched elements, we observe a more clustered picture, with a mean of 6.6 mm (1.8 mm of standard deviation). Retouched and unretouched blanks display an asymmetric distribution and are statistically different (Mann-Whitney, T=UB=1392, $p < 0.01$) (figs. 18 & 19).

Platforms are plain and show oblique external platform angle, the internal ridge of the platform is lipped and the external ridge of the platform shows traces of abrasion. When looking at the profile of laminar blanks, we observe a similar trend as the one described on the larger sample from Unit G (figs. 20 & 21). Bl-

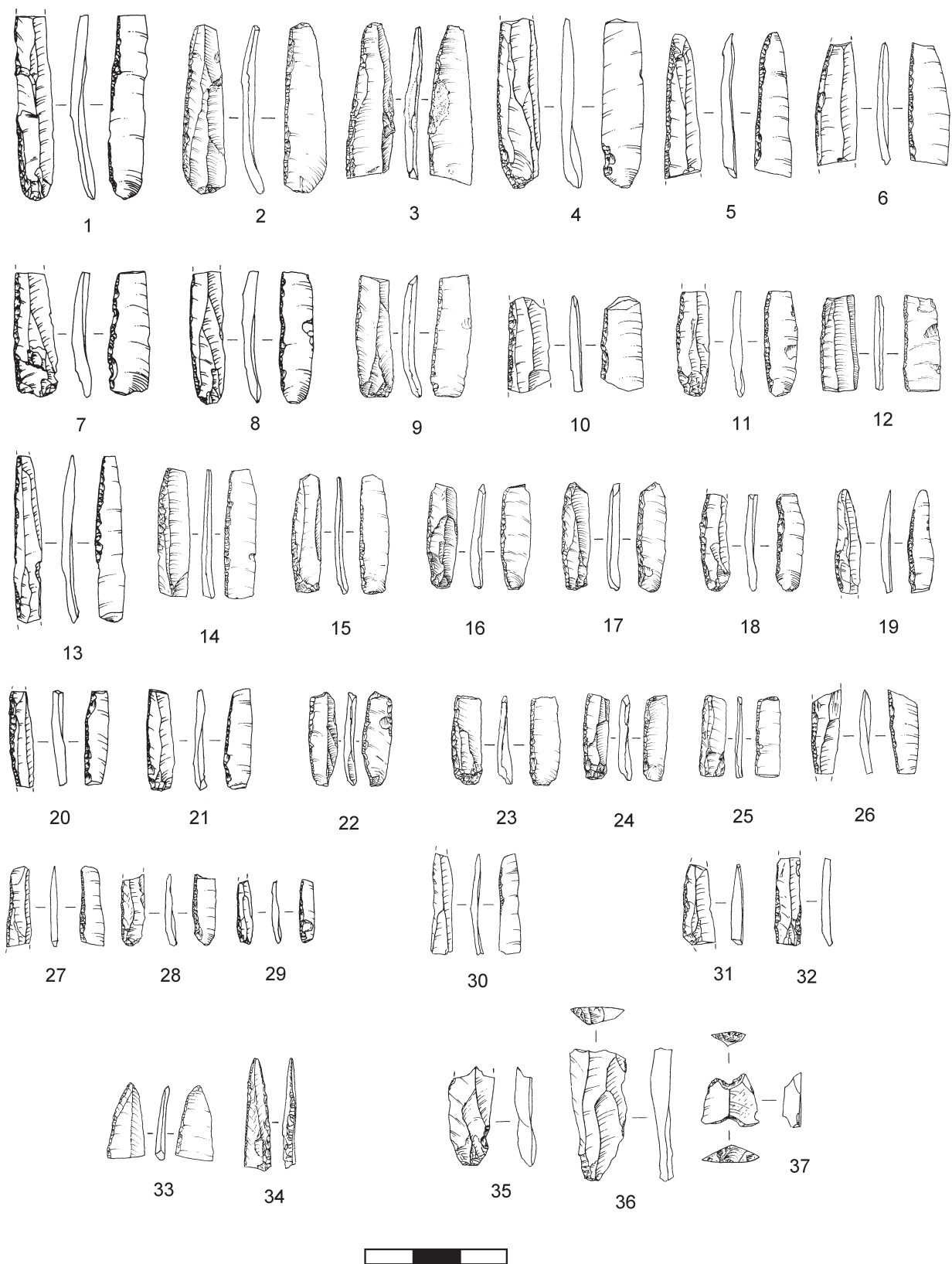


Figure 16 - Retouched bladelets and microblades from sub-levels Gc1 and Gc2 (illustrations borrowed with the courtesy of Yu. E. Demidenko).

adelets show a trend toward curved profiles, although straight profiles are also well represented. The unretouched bladelets, together with the retouched and unretouched microblades, tend to be straight. Dorsal scars are unidirectional and most of the time convergent. Sections are trapezoidal or sometimes triangular.

The retouch location is mainly alternate. Inverse retouch is also well represented (fig. 8). Retouched bladelets and microblades are mainly Dufour, with one complete bladelet and two bilaterally retouched distal fragments typed as Font-Yves/Krems. One fragment is pointed by bilateral steep retouch. In addition,

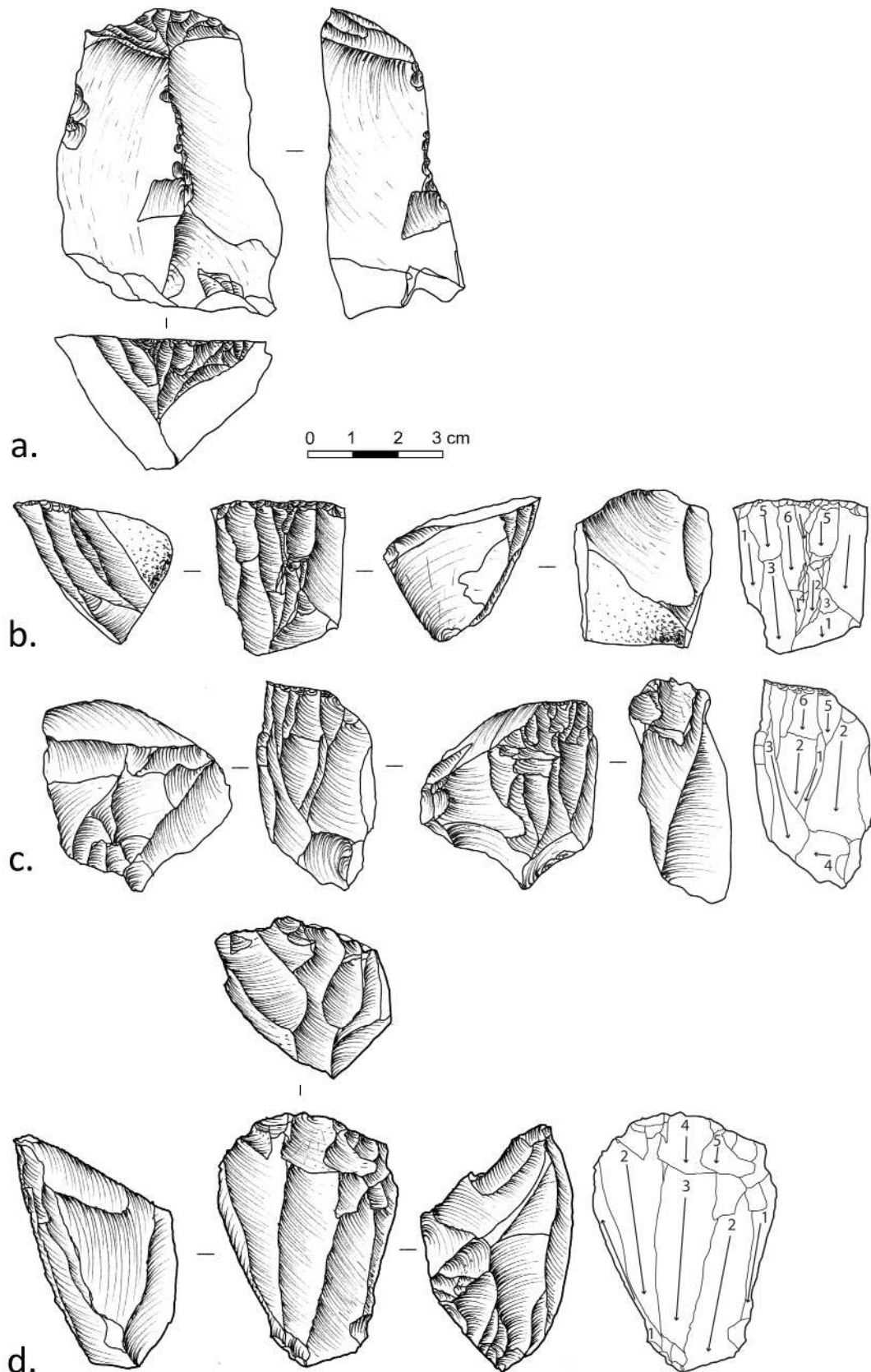


Figure 17 - Unit H, Cores and diacritic reconstruction. The different phases illustrate the chronology of removals (drawing by N. Zwyns).

one proximal bilaterally retouched fragment could be associated to this type. One retouched Dufour show a micro-spall removal from the tip that could be interpreted as evidence of impact.

Summary

The bladelet and microblade production from sub-levels Fb1 and Fb2 show numerous similarities, from the blank produc-

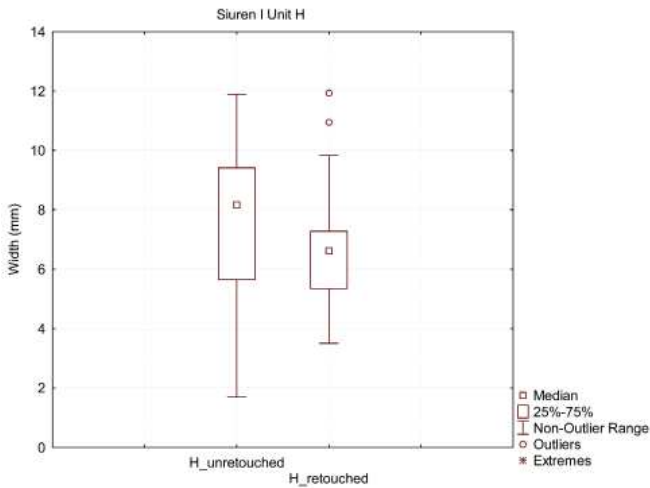


Figure 18 - Box-plot comparing the width distribution of unretouched and retouched elements from Unit H. Whiskers are drawn from the top of the box up to the largest data point less than 1.5 times the box height (upper inner fence). The circles represent values which are outside the upper inner fence, considered here as outliers.

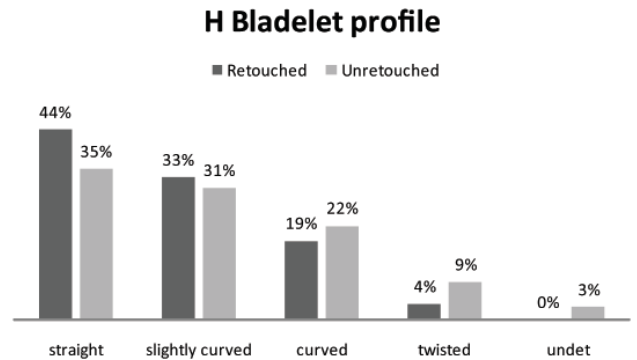
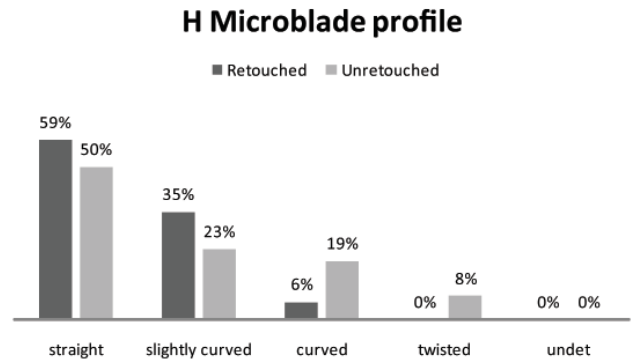


Figure 20 - Unit H, laminar element profiles.

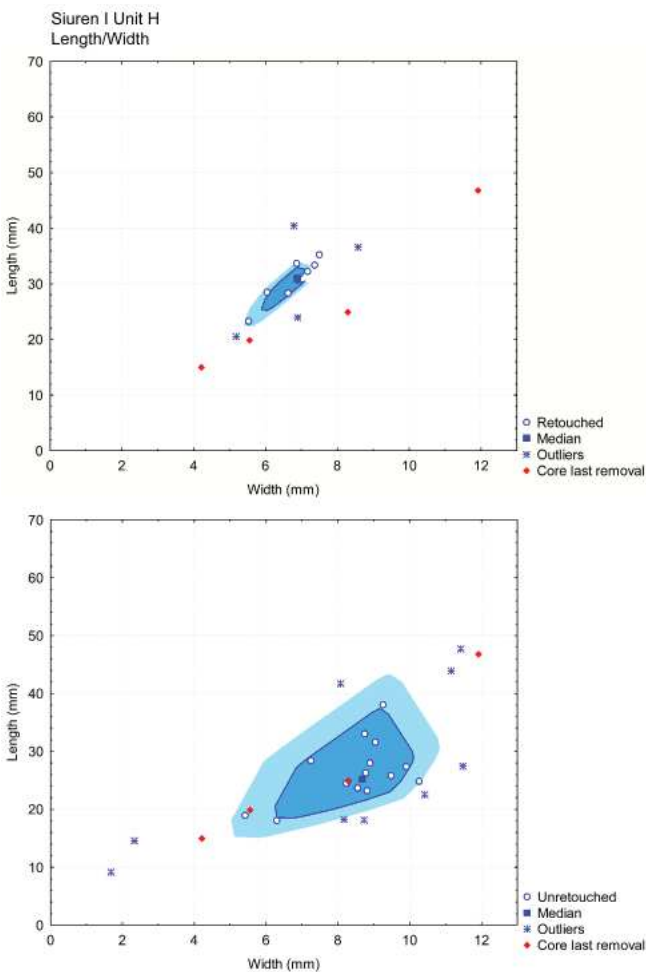


Figure 19 - Bag-plot chart showing the length/width distribution of retouched and unretouched elements from Unit H, compared with the complete last removals observed on the cores. The dark circle (bag) represent 50% of the observations with greatest bivariate depth. The light circle (loop) represent three times the bag (fence).

tion to their retouched elements. The use of burins as cores is one element to be underlined. These forms of burins include carinated burins and one busked burin. Some of the last removals are clearly twisted and off-axis. The *debitage* is mainly unidirectional and convergent. Retouched elements from Fb1 and Fb2 show a symmetrical distribution in terms of width, the two groups being statistically analogous (fig. 22) (Mann-Whitney, $T=UB=412, p=0.6$). It suggests a goal of blank production with a mean of 6mm width which after secondary treatment is narrowed around 4.8 mm. If we ignore the noise caused by outliers and extreme measurements, median values are even lower. If we consider the microblade category starting at 7 mm, it is interesting to see that in sub-level Fb1, only one bladelet has been retouched. If retouched elements are in majority on off-axis blanks, sub-level Fb1 is balanced in terms of profiles. Twisted profiles are dominant, but closely followed by other categories. However, a large majority of retouched elements from Fb2 are on twisted blanks, including Dufour of *Roc-de-Combe* subtype. This uneven situation could be linked to sampling effect, an unidentified functional pattern in this part of the site, but also to the desired morphology of the blank. By trying to produce off-axis blanks from carinated burins or carinated endscrapers, one might increase the number of twisted elements produced. In other words, twisted profiles may not be as important a feature as the off-axis character. We also note the absence of the Font-Yves type among the retouched elements, and the occurrence of three partially backed microblades in Fb1.

In comparison, Unit G⁴ and H show a very different picture. Carinated burins are totally absent. The only burins from these

⁴ As noted above, we consider here sub-levels Gc1-Gc2 as representative of the entire Unit G, other sub-levels yielding similar results.

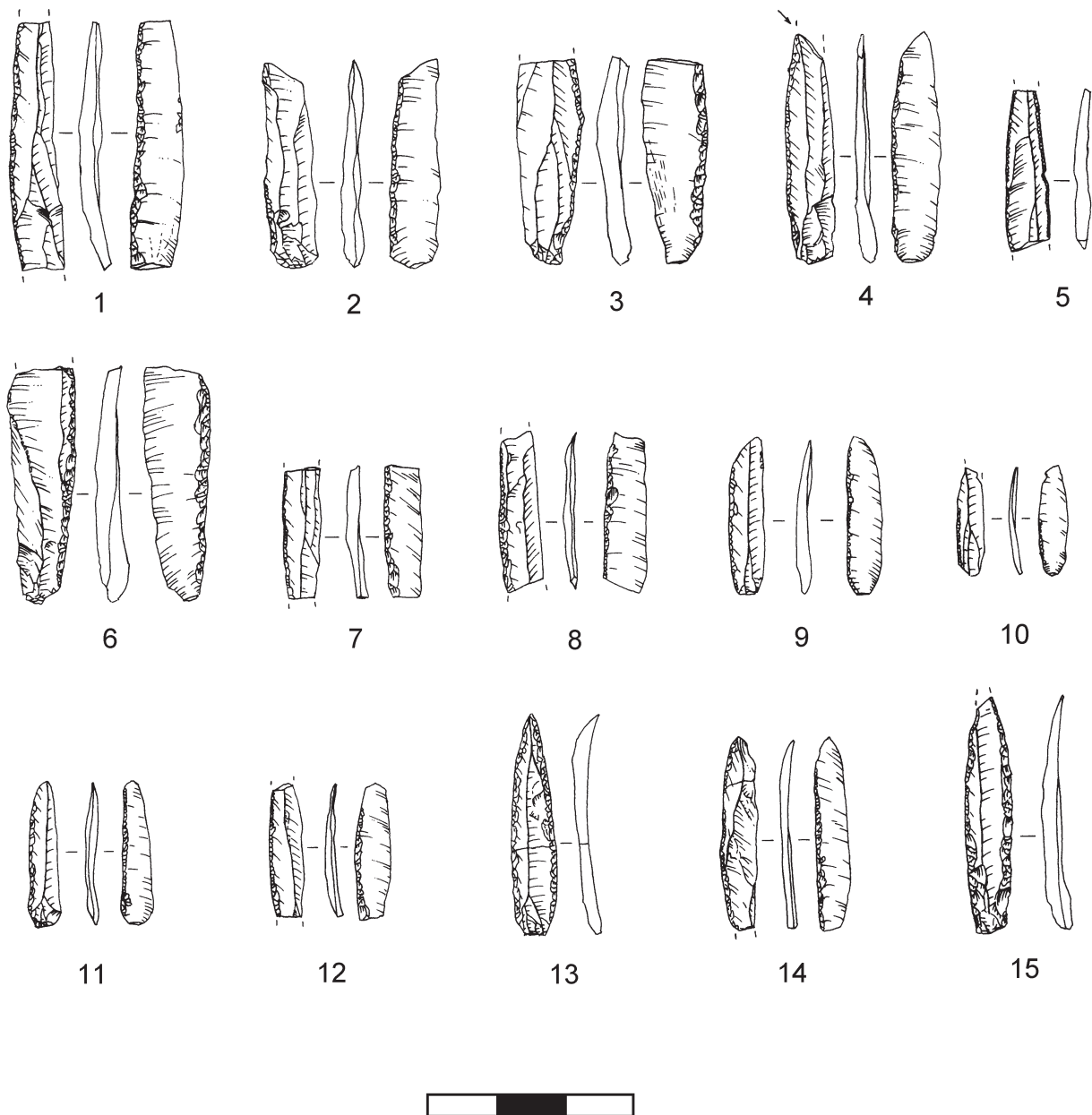


Figure 21 - Retouched bladelets and microblades from Unit H (illustrations borrowed with the courtesy of Yu. E. Demidenko).

samples are mainly *burin d'angle* or on truncation. Cores are unidirectional with a triangular flaking surface tending to convergence. Some of the cores show a carinated endscraper morphology with a broad flaking surface. The largest one shows removals overlapping with the size of the largest laminar elements. Smaller carinated elements are also associated with these units, their last removals falling into the range of the microblade category. From a more general point of view, the frequency of cores is rather low.

Laminar blanks show a trend toward the production of straight microblades bearing alternate or inverse retouch, the latter systematically along on the right edge (almost 100% for both Gc1-Gc2 and H). These are typologically attributed to Dufour. Although outliers are easily noticed, the median of width is relatively small. We note the presence of pointed bladelets and

microblades. Clear Font-Yves/Krems points have been recognized, a few bilaterally retouched mesio-distal or distal fragments being highly similar. At least three distal fragments of Dufour microblade underline the pointed morphology of some of these tools when the latter is observable. We also note the presence of an asymmetrical point similar to those found in Proto-Aurignacian context, as at Le Piage, or Fumane (Broglio *et al.* 2005; Bordes *et al.* 2010) and some intermediate Font-Yves tips showing bilateral steep retouch.

The morphology of unit H retouched elements is similar to unit G, tending clearly toward slightly curved or straight profiles, with alternate or inverse retouch.

When we compare the retouched blanks from Unit G with the sample from Fb2, we observe significantly different with distri-

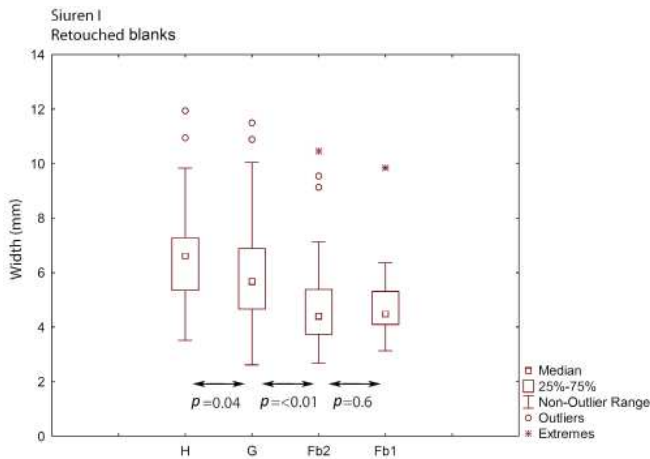


Figure 22 - Box-plot showing a general comparison of the width between the sub-levels and Unit studied, with p-values of Mann-Whitney U-test. Results are considered significant when <0.01 0-hypothesis assumes a symmetric distribution. Whiskers are drawn from the top of the box up to the largest data point less than 1.5 times the box height (upper inner fence). The circles represent values which are outside the upper inner fence, considered here as outliers.

butions (Mann-Whitney, $T=UB=1467$, $p=<0.01$) (fig. 22). However, when compared, Fb1 and Fb2 retouched element widths are similar. Unit G and unit H samples also show comparable distributions although unit G blanks tend to be slightly narrower (Mann-Whitney, $T=UB=1680$, $p=0.04$)⁵. In other words, based on the width, the largest set of retouched elements from Fb1-Fb2 and G-H variants are significantly different from each other. Nevertheless, Fb1 is analogous to Fb2 and G is analogous to H. These observations are confirmed when looking at the width means differences ($F(3, 210) = 11.7$, $p = <0.01$). Tukey's pairwise comparisons underline the similarities between units Fb1 and Fb2 and between units G and H while showing significant differences between those two groups. The difference between Fb1 and Gc appear significant only with a 96% level of confidence, level G tending to have numerous small size blanks.

Sub-levels Fb1 and Fb2 are oriented toward the production of smaller blanks that are most of the time slightly retouched, making the width difference between unretouched and retouched elements less sharp than in the case of Unit G or Unit H. In these assemblages, the metric attributes of the blanks are less clustered. This variability is balanced by an intensive and systematic alternate retouch which tends to crop the blank.

Discussion

The differences expressed in terms of bladelets and microblades between units Fb1-Fb2 and G-H have to be understood in the context of a technological change in hafting strategies. It is very likely that such elements take part in composite objects for which we are missing the organic component. As observed in different chronological contexts, the general aspect of a lithic assemblage is strongly influenced by the morphology of point-

⁵ Although the null-hypothesis can be rejected with a 95% level of confidence ($p=<0.05$).

	Fb1	Fb2	Gc	H
Fb1	0	0.99	0.04	<0.01
Fb2	0.46	0	0.01	<0.01
Gc	3.78	4.24	0	0.44
H	5.91	6.37	2.12	0

Table 3 - Tukey's pairwise comparisons (p-values are in the upper right corner)

ed elements. In other words, the morphological attributes of the lithic component in hunting weapons will shape part of the lithic assemblage. In this view, the Fb1-Fb2 assemblage seems driven by the need to produce off-axis microblades, concomitantly displaying twisted profiles. One of the technological options to obtain such blanks is to use the narrow edge of a flake or laminar blank, giving to it a burin-like morphology. They differ from those considered as tools mainly by their lack of sharp edges and the multiple removals on their flaking surface.

Such elements are entirely absent from Units G and H, where the focus is more on straight blanks. The only carinated elements in the sample are endscrapers. Thick or short endscrapers yield similar blanks, with only variation in size. In the absence of long refit sequences, it is not possible to observe any clear continuity between the blade and the bladelet/microblade production.

One of the important observations made is that both Fb1-Fb2 and G-H assemblages are mainly characterized by the production of microblades rather than bladelets. Although blade production was not analyzed here, we could not find any evidences of a continuum in their production in Unit Fb1-Fb2. Looking at the Fb1 unretouched element width values, we can observe that the curve show a positive skew (skewness: 0.7) (fig. 23). The frequency decreases as we approach the 12 mm cut-off. It thus seems rather likely that both blade and bladelet/microblade groups would yield a bimodal distribution.

The same histogram shows different results for Units G and H (fig. 24). The artificial cut-off is highly visible among unretouched elements, the negative skew implying a possible link with blade production (e.g. Gc1-Gc2 skewness: -0.2). In general, retouched elements show a positive skew and a more clustered picture (e.g. Gc1-Gc2 skewness: 0.8), reflecting a reduction of the width by retouch. Among the cores observed, only one from Unit H shows a possible link between these two productions, being between the two categories at the time of discard. In spite of a significant occurrence of blade and technical flakes within both assemblages, blade cores remain absent. However, we observe that some cores illustrate an independent reduction sequence. Therefore, the continuum between blades and bladelets (if there is any), is not the only way leading to the small-sized blanks.

Although this material will be put into context in the forthcoming chapters, some contextual remarks can be formulated here. From a regional point of view, the sample from Fb1 display similarities the material from the Aurignacian from Kostenki 14 volcanic ash level. Although showing older radiometric dates, the assemblage is also oriented on the production of microblades, rather than bladelets, but with slightly curved or curved

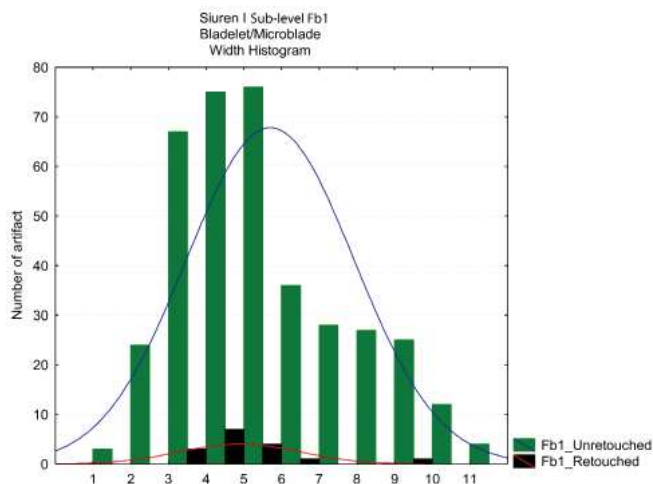


Figure 23 - Sub-level Fb1, histogram of the width values of retouched and unretouched elements.

profiles (Sinitsyn 2003a). The Aurignacian I from Mitoc-Malu Galben also shows technological affinities with this assemblage although no retouched microliths could be identified in the small sample studied (Noiret 2005; Noiret *et al.* in press).

Unit Fb2 could fit in the same comparison, although the discrete occurrence of busked burin is noteworthy. This type of artifact is almost absent in any Central European Aurignacian assemblages, but clearly associated with the Evolved Aurignacian in Western and North-Western Europe (Chiotti 2003; Flas *et al.* 2006). Recently, similar artifacts have been reported in the assemblage from Kostenki 14 level VIb. However, this assemblage shows an unusual association between Aurignacian technology and bifacial elements (Sinitsyn 2003b).

Units G and unit H, as previously observed (Demidenko 2001; Demidenko & Otte 2001; Demidenko 2008a), display a high degree of technological and typological similarity with the Proto-Aurignacian from Western Europe. This comparison is reinforced by the results of this analysis, bladelet and microblade technology being one of the main criteria to identify this techno-complexes. The Early Kozarnikian, although associated with dates around 38 kyr is the most comparable assemblage in the area. Apart from this example, Proto-Aurignacian remains poorly documented in Eastern Europe (Tsanova 2008). Some reworked material from the north-eastern shore of the Black Sea (Kamennomostskaya lower layer, Shyrokiy Mys) could represent evidence for similar occupations, although the absence of a clear chronological and stratigraphic context sharply limits possibilities of comparison (Demidenko 2001; Demidenko & Otte 2001; Demidenko 2008a).

From a technological perspective, the analogy with the European Proto-Aurignacian (Units G-H) and the Recent Aurigna-

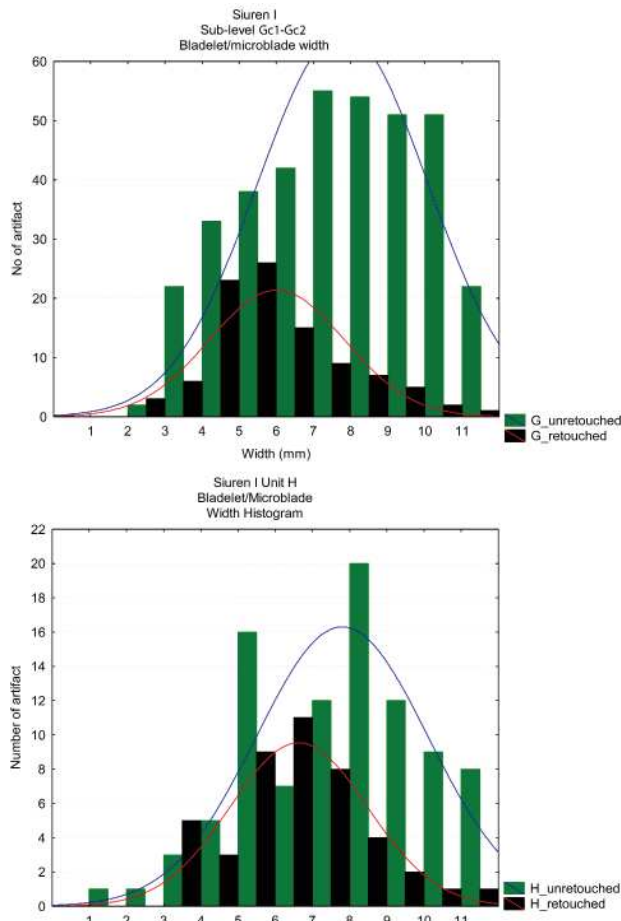


Figure 24 - Sub-level Fb1, histogram of the width values of retouched and unretouched elements.

cian is the most relevant (Fb1-Fb2). In this context, Siuren 1 is one of the key sites in Eastern Europe as it displays these two variants in a single sequence. Although the radiometric dates seem slightly younger than the neighboring Aurignacian sites, the Fb1-Fb2 unit fits with the expected range of the Evolved Aurignacian, and certainly not with a Late Glacial Maximum industry (Zwyns 2004). The Proto-Aurignacian attribution mainly relies on the techno-typological attribution of the collection, and on its stratigraphic location. As will be discussed in more detail in the comparison chapter, we believe that this attribution remains the most likely.

Acknowledgments

The author is grateful to Y. Demidenko for the preparation and the access to the material, to Y. Demidenko, P.R. Nigst, R. Ioviță and S.P. McPherron for discussion and advice on the writing of this chapter, to R. Miller for helping with the translation and to J.-J. Hublin and the Max Planck Society for their financial support.